









Eco-friendly synthesis, antimicrobial activity, molecular docking and ADMET studies of novel α -aminophosphonates

Sumithra Poreddy ¹, Mohan Gundluru ¹, Santhisudha Sarva ¹,
Surenra Pothuraju ², Poojitha Bellala ¹,
Kranthi Kumar Konidala ³, Suneetha Yeguvapalli ⁴
and Suresh Reddy Cirandur ^{1*}

¹Department of Chemistry, Sri Venkateswara University, Tirupati-517 502, A.P., India

²Department of Chemistry, School of Advanced Sciences, VIT, Vellore - 632 014. T.N., India

³Research Associate (ICMR), Bioinformatics, Department of Zoology, Sri Venkateswara University, Tirupati-517 502, A.P., India

⁴Department of Zoology, Sri Venkateswara University, Tirupati-517 502, A.P., India

(Received July 20, 2024; Revised September 19, 2024; Accepted September 23, 2024)

Abstract: An efficient one-pot Kabachnik-Fields reaction has been carried out for the synthesis of novel α -aminophosphonates under microwave irradiation and solvent-free conditions by 2-hydroxy-1-naphthaldehyde, aromatic amines and dialkyl phosphites using Hydroxyapatite nanoparticles (HAp NPs) as catalyst. The present new protocol is environmentally benign as it offers some interesting and promising features like solvent-free, low cost, safety, minimal waste, atom efficiency, easy work-up, short reaction time and possessing excellent functional group tolerance to structurally diverse derivatives. The title compounds were subjected to antimicrobial activity against bacterial and fungal strains by disc diffusion and MIC methods. Advanced computational tools were also employed to conduct molecular docking and toxicogenomic investigations on target compounds. Employing ensemble-docking approaches, the primary contenders were identified for their potential to bind to the active sites of GlcN-6-P synthase, with PDB IDs 2VF5 and 2POC acting as target receptors. ADMET studies revealed promising drug-like characteristics of these compounds.

Keywords: α -Aminophosphonates; HAp NPs; microwave irradiation; solvent-free synthesis; antimicrobial activity; ADMET. ©2024 ACG Publication. All right reserved.

1. Introduction

Organophosphorus compounds have numerous applications in various fields like agriculture and medicine¹. Organophosphorus compounds are used as pesticides for plants and animals and their positive contribution leads to efficient food production and fighting against diseases like malaria, yellow fever and typhus². Phosphorus analogues have important potential catalytic activity and iron carrier properties in supramolecular and synthetic organic chemistry³⁻⁵. Phosphorous-containing macrocyclic molecules serve as effective hosts in host-guest chemistry, this property makes it possible for them to transport drug molecules to the necessary location in living organisms⁶⁻⁷. They are also

* Corresponding author: E-Mail: csrsvu@gmail.com

used to investigate the mechanism of cADPR-mediated Ca^{2+} signaling pathways and are anticipated to be used as leads for the development of potential drugs, indicating a bright future for the pharmaceutical industry⁸⁻¹⁰. The synthesis of α -aminophosphonates has attracted much attention because they act as building blocks of peptides, as α -aminophosphonates seem to be closer analogues of α -amino acids than their α -aminophosphoric counterparts due to their monobasic/acidic character and the high stability of P-C bond of phosphonic acids compared with the P-O bond¹¹⁻¹². They also act as enzyme inhibitors¹³⁻¹⁴, haptens of catalytic antibodies¹⁵, antimicrobial agents¹⁶⁻¹⁷, anticancer agents¹⁸⁻²⁰, antioxidants, anti-inflammatory and anti-Alzheimer agents²¹⁻²⁵, antivirals²⁶⁻²⁷, antidiabetic²⁸ and plant growth regulators in agro chemistry²⁹⁻³².

As the development of an efficient and convenient method for the synthesis of α -aminophosphonates by Kabachnik-Fields reaction is of great significance and highly desirable³³⁻³⁵. In the Kabachnik-Fields reaction for synthesizing α -aminophosphonates, numerous catalytic methods have been explored, involving diverse acids³⁶⁻³⁸, nano-materials³⁹⁻⁴⁵ and ionic liquids⁴⁶⁻⁵⁰ as catalysts. However, existing protocols suffer from drawbacks, including prolonged reaction times, the utilization of costly and hazardous chemicals, harsh reaction conditions and suboptimal product yields. Consequently, there is an imperative need to devise a more effective, straight forward and environmentally friendly approach for generating α -aminophosphonate derivatives with higher yields. As a part of our program, we aimed at developing efficient and environmentally friendly products and we continue our effort to achieve that we would like to report herein a facile and efficient method for the synthesis of α -aminophosphonates *via* one pot Kabachnik-Fields reaction of 2-hydroxy-1-naphthaldehyde with various substituted aromatic/heteroaromatic amines and dialkyl phosphites under microwave irradiation and solvent free conditions.

In recent years, Hydroxyapatite nanoparticles (HAP NPs) have garnered considerable interest in many areas and it has properties such as ion-exchange ability, adsorption capacity, acid-base properties and efficient catalytic activity in organic reactions⁵¹⁻⁵⁴. The small size of HAP NPs as one of the important biocompatible and bioactive materials with higher surface areas and lower particle sizes can provide greater catalytic activity in organic synthesis⁵⁵⁻⁵⁷. Hence, we designed novel α -aminophosphonate derivatives *via* one-pot three-component condensation reaction, as this became preferred protocol and was used extensively for synthesizing new heterocyclic compounds due to its simple set-up procedure, reduced reaction time, excellent yields and reduced pollutant production.

Opportunistic bacterial and fungal infections are a significant contributor to morbidity and mortality in immunocompromised individuals⁵⁸. There has been a notable rise in the occurrence of invasive bacterial and fungal infections over the past ten years⁵⁹. To address these challenges, the development of novel drug candidates that are safe and exhibit high selectivity while minimizing toxicity is urgently needed. Glucosamine-6-phosphate synthase (GlcN-6-P synthase, L-glutamine:D-fructose-6-P amido transferase) has emerged as a new target for antibacterial⁶⁰ and antifungal⁶¹ agents. GlcN-6-P synthase initiates hexosamine metabolism by converting fructose 6-phosphate to glucosamine-6-phosphate (GlcN-6-P) using glutamine. This enzymatic reaction, which is irreversible in nature, represents the binding step in the pathway. *N*-acetyl glucosamine, the end product of the pathway, serves as a key building block for bacterial and fungal cell walls. Variations in structure between prokaryotic, fungal and human enzymes have been used to design customized inhibitors, paving the way for the development of antifungal and antibacterial pharmaceutical agents⁶². In addition, the ADMET properties (absorption, distribution, metabolism, excretion, and toxicity) along with the drug likeness were evaluated.

Considering the above results, we describe the synthesis and antimicrobial properties of novel α -aminophosphonate derivatives. From this research, we conducted molecular docking studies on biologically active compounds to gain a thorough understanding of drug receptor interactions.

2. Experimental

2.1. Chemical Material and Apparatus

All reactions were carried out by using oven-dried glassware. All necessary chemicals and solvents were purchased from Sigma-Aldrich and used without purification. The catalyst HAP NPs is

Synthesis and antimicrobial activity of novel α -aminophosphonates

purchased from Sisco Research Laboratories Pvt. Ltd. Mumbai, India. Microwave irradiation (MWI) was conducted using a scientific microwave catalyst system (CATA-4R). The purity of the products and progress of the reaction was confirmed by thin layer chromatography on pre-coated silica gel plates purchased from Merck. Visualization was done under UV light and iodine chamber. Melting points were determined in open capillary tube on EZ-Melt Automated Melting Point Apparatus and are uncorrected. IR spectra were recorded as neat samples on Bruker Alpha-Eco ATR-FTIR (Attenuated Total Reflection-Fourier Transform Infrared) interferometer with single-reflection sampling module equipped with Zn-Se crystal, the data was expressed in reciprocal centimetres (cm^{-1}). NMR spectra were recorded on JEOL (400 MHz) NMR spectrometers operating at 400 MHz for ^1H NMR, 100 MHz for ^{13}C NMR and 161.9 MHz for ^{31}P NMR. Data were recorded in CDCl_3 which referenced to TMS (^1H NMR and ^{13}C NMR), 85% H_3PO_4 (^{31}P NMR). Assignments of the signals were based on the chemical shifts and intensity patterns. Chemical shift (δ) and coupling constant (J) were expressed in ppm and Hertz respectively. Liquid chromatography- mass spectra were recorded on Micro mass Q-TOF micro mass spectrometer using electro spray ionization.

2.2. Chemistry

2.2.1. General Procedure for the Synthesis of α -aminophosphonates **4a-j** by Conventional Method

A solution containing 2-hydroxy-1-naphthaldehyde (**1**, 1 mmol), various aromatic amines (**2a-e**, 1 mmol), dialkyl phosphites (**3a-b**, 1 mmol), and HAp NPs (7.5 mol%) is prepared in a 50 ml round-bottom flask and stirred at room temperature. At ambient temperature the progress of the reaction is observed using TLC analysis. Following the reaction's completion, the resulting residue is subjected to purification *via* column chromatography on silica gel, employing hexane:ethyl acetate as an eluent to yield the pure products **4a-j**^{22,63}.

2.2.2. General Procedure for the Synthesis of α -aminophosphonates **4a-j** by Microwave Method

A solution containing 2-hydroxy-1-naphthaldehyde (**1**, 1 mmol), various aromatic amines (**2a-e**, 1 mmol), dialkyl phosphites (**3a-b**, 1 mmol) and HAp NPs (7.5 mol%) is prepared in a flat-bottom flask and subjected to microwave irradiation (MWI) using (CATA-4R) at 200 W. The completion of the reaction was observed by TLC using hexane:ethyl acetate every minute. The reaction reached completion within 3 minutes. Upon completion, the mixture was dissolved in 10 ml of dichloromethane (DCM) and filtered to remove the catalyst residue. The organic layer was washed with water and the aqueous layer was discarded. After that, the combined organic mixture was dried over anhydrous Na_2SO_4 and concentrated under low pressure after being cleaned with a brine solution. The resulting solids were washed with cold water, air-dried and recrystallized from ethanol to obtain the pure compounds^{16,64}.

2.3. Spectral Data of Representative Compounds

Diethyl ((2-hydroxynaphthalen-1-yl)((6-methylpyridin-2-yl)amino)methyl)phosphonate (4a): Dark Red solid, Yield: 95%, mp: 138-139 °C. FTIR (neat) ($\nu_{\text{max}}/\text{cm}^{-1}$): 3362 (NH), 1251 (P=O), 1018 (P-O-C), 793 (P-C); ^1H NMR: (CDCl_3 , 400 MHz), δ 10.53 (s, 1H, OH), 7.64-7.52 (m, 2H, Ar-H), 7.09 (t, $J_1 = 8.0$ Hz, $J_2 = 8.0$ Hz, 2H, Ar-H), 6.91 (d, $J = 8.0$ Hz, 2H, Ar-H), 6.68-6.62 (m, 3H, Ar-H), 5.41 (d, $J = 24$ Hz, 1H, P-CH), 4.93 (s, 1H, CH-NH), 4.54-3.82 (m, 4H, O-CH₂-CH₃), 2.72 (s, 3H, CH₃), 1.35 (t, $J_1 = 8.0$ Hz, $J_2 = 4.0$ Hz, 3H, O-CH₂-CH₃), 1.29 (t, $J_1 = 8.0$ Hz, $J_2 = 4.0$ Hz, 3H, O-CH₂-CH₃) ppm; ^{13}C NMR (CDCl_3 , 100 MHz), δ 162.44, 161.05, 159.03, 155.19, 133.89, 127.87, 127.13, 122.52 (d, $J = 9$ Hz), 121.03, 116.08, 115.83, 115.61, 114.54, 114.47, 113.19, 111.45, 63.31-63.22 (m), 48.70 (d, $J = 153$ Hz), 16.25 (d, $J = 7$ Hz), 14.41 ppm; ^{31}P NMR (CDCl_3 , 161.9 MHz), δ 23.42 ppm; LCMS (ESI): m/z calculated for $\text{C}_{21}\text{H}_{25}\text{N}_2\text{O}_4\text{P}$: $[\text{M}+\text{H}]^+$ 401.2823, found 401.2820.

Diethyl ((2-hydroxynaphthalen-1-yl)((4-methoxyphenyl)amino)methyl)phosphonate (4b): Brown solid, Yield: 95%, mp: 138-139 °C. FTIR (neat) ($\nu_{\text{max}}/\text{cm}^{-1}$): 3367 (NH), 1240 (P=O), 1029 (P-O-C), 782 (P-C); ^1H NMR: (CDCl_3 , 400 MHz), δ 10.52 (s, 1H, OH), 7.78-7.61(m, 4H, Ar-H), 6.89 (d, $J = 4.0$ Hz,

2H, Ar-H), 6.67 (d, $J = 8.0$ Hz, 2H, Ar-H), 6.58 (d, $J = 8.0$ Hz, 2H, Ar-H), 5.36 (d, $J = 28.0$ Hz, 1H, P-CH), 5.02 (s, 1H, CH-NH), 4.52-3.90 (m, 4H, OCH₂) 3.66 (s, 3H, O-CH₃) 1.35 (t, $J_1 = 8.0$ Hz, $J_2 = 4.0$ Hz, 3H, O-CH₂-CH₃), 1.29 (t, $J_1 = 8.0$ Hz, $J_2 = 4.0$ Hz, 3H, O-CH₂-CH₃) ppm; ¹³C NMR (CDCl₃, 100 MHz), δ 165.78, 163.60, 162.44, 159.03, 157.54, 155.19, 133.89, 127.87, 127.13, 122.52 (d, $J = 9$ Hz), 121.03, 115.95, (d, $J = 25.0$ Hz), 115.61, 114.54, 114.47, 113.19, 63.3 (d, $J = 2.0$ Hz), 63.23 (d, $J = 2.0$ Hz), 48.70 (d, $J = 153.0$ Hz), 28.50, 16.54 (d, $J = 6.0$ Hz), 16.25 (d, $J = 7.0$ Hz) ppm; ³¹P NMR (CDCl₃, 161.9 MHz) δ 22.85 ppm; LCMS (ESI): m/z calculated for C₂₂H₂₆NO₅P: [M+H]⁺ 416.5186, found 416.5183.

Diethyl ((2-hydroxynaphthalen-1-yl)(pyrimidin-2-ylamino)methyl)phosphonate (4c): Orange solid, Yield: 95%, mp: 138-139 °C. FTIR (neat) (v_{\max}/cm^{-1}): 3365 (NH), 1250 (P=O), 1019 (P-O-C), 792 (P-C); ¹H NMR: (CDCl₃, 400 MHz), δ 10.52 (s, 1H, OH), 8.02 (m, 1H, Ar-H), 7.86 (d, $J = 8.0$ Hz, 2H, Ar-H), 7.06 (d, $J = 12$ Hz, 2H, Ar-H), 6.91 (m, 2H, Ar-H), 6.80 (m, 1H, Ar-H), 6.76-6.54 (m, 3H, Ar-H), 5.32 (d, $J = 28$ Hz, 1H, P-CH), 4.80 (s, 1H, CH-NH), 4.36-3.76 (m, 4H, O-CH₂), 1.35 (t, $J_1 = 4.0$ Hz, $J_2 = 8.0$ Hz, 3H, O-CH₂-CH₃), 1.29 (t, $J_1 = 4.0$ Hz, $J_2 = 8.0$ Hz, 3H, O-CH₂-CH₃) ppm; ¹³C NMR (CDCl₃, 100 MHz), δ 162.50, 161.04, 158.97 (d, $J = 6$ Hz), 145.86 (d, $J = 14$ Hz), 139.19, 129.33, 127.87 (d, $J = 3$ Hz), 127.12 (d, $J = 4.0$ Hz), 121.11, 119.91, 111.55 (t, $J_1 = 27.0$ Hz, $J_2 = 2.0$ Hz), 63.49 (d, $J = 7$ Hz), 63.34 (d, $J = 7$ Hz), 49.79, 48.25, 16.61 (d, $J = 5$ Hz), 16.36 (d, $J = 6.0$ Hz) ppm; ³¹P NMR (CDCl₃, 161.9 MHz) δ 22.35 ppm; LCMS (ESI): m/z calculated for C₁₉H₂₂N₃O₄P: [M+H]⁺ 388.5440, found 388.5437.

Diethyl ((2-hydroxynaphthalen-1-yl)((5-nitropyridin-2-yl)amino)methyl)phosphonate (4d): Brown solid, Yield: 94%, mp: 138-139 °C. FTIR (neat) (v_{\max}/cm^{-1}): 3362(NH), 1247 (P=O), 1079 (P-O-C), 772 (P-C); ¹H NMR: (CDCl₃, 400 MHz), δ 10.70 (s, 1H, OH), 8.14 (s, 1H, Ar-H), 8.01 (d, $J = 8.0$ Hz, 1H, Ar-H), 7.95 (s, 1H, Ar-H), 7.38-7.14 (m, 6H, Ar-H), 5.52 (d, $J = 20$ Hz, 1H, P-CH), 4.86 (s, 1H, CH-NH), 4.09-3.57 (m, 4H, O-CH₂), 1.33 (t, $J_1 = 8.0$ Hz, $J_2 = 4.0$ Hz, 3H, O-CH₂-CH₃), 1.20 (t, $J_1 = 8.0$ Hz, $J_2 = 8.0$ Hz, 3H, O-CH₂-CH₃) ppm; ¹³C NMR (CDCl₃, 100 MHz), δ 155.61, 146.27, 140.24, 137.11, 125.86 (d, $J = 9$ Hz), 125.64 (d, $J = 6.0$ Hz) 122.91 (d, $J = 4.0$ Hz), 120.61 (d, $J = 9.0$ Hz), 120.09, 118.90, 63.22 (d, $J = 4.0$ Hz), 63.10 (d, $J = 7.0$ Hz), 54.21 (d, $J = 7.0$ Hz), 53.18 (d, $J = 154$ Hz), 37.58, 16.41 (d, $J = 6.0$ Hz), 16.19 (d, $J = 6.0$ Hz) ppm; ³¹P NMR (CDCl₃, 161.9 MHz) δ 20.97 ppm; LCMS (ESI): m/z calculated for C₂₀H₂₂N₃O₆P: [M+H]⁺ 431.1357, found 431.1353.

Diethyl (((3-chloro-4-fluorophenyl)amino)(2-hydroxynaphthalen-1-yl)methyl)phosphonate (4e): Brown solid, Yield: 95%, mp: 138-139 °C. FTIR (neat) (v_{\max}/cm^{-1}): 3368 (NH), 1259 (P=O), 1016 (P-O-C), 782 (P-C); ¹H NMR: (CDCl₃, 400 MHz), δ 10.84 (s, 1H, OH), 7.76-7.64 (m, 6H, Ar-H), 6.96 (s, 1H, Ar-H), 6.73 (d, $J = 8.0$ Hz, 1H, Ar-H), 6.57 (d, $J = 8.0$ Hz, 1H, Ar-H), 5.11-5.08 (dd, $J_1 = 8.0$ Hz, $J_2 = 4.0$ Hz, 1H, P-CH), 4.85 (s, 1H, CH-NH), 4.38-3.76 (m, 4H, OCH₂), 1.33-1.25 (m, 6H, O-CH₂-CH₃) ppm; ¹³C NMR (CDCl₃, 100 MHz), δ 159.05, 151.51, 142.35, 133.53 (d, $J = 7.0$ Hz), 131.68, 130.57 (d, $J = 8.0$ Hz), 128.79, 122.17 (d, $J = 5.0$ Hz), 117.72, 113.12, 110.26, 108.62, 63.25 (d, $J = 4.0$ Hz), 63.16 (d, $J = 4.0$ Hz), 43.27 (d, $J = 12.0$ Hz), 16.32 (t, $J_1=7.0$ Hz, $J_2=8.0$ Hz) ppm; ³¹P NMR (CDCl₃, 161.9 MHz) δ 22.11 ppm; LCMS (ESI): m/z calculated for C₂₀H₂₂N₃O₆P: [M+H]⁺ 438.5295, found 438.5292.

Dimethyl ((2-hydroxynaphthalen-1-yl)((6-methylpyridin-2-yl)amino)methyl)phosphonate (4f): Brown solid, Yield: 94%, mp: 138-139 °C. FTIR (neat) (v_{\max}/cm^{-1}): 3340 (NH), 1220 (P=O), 1012 (P-O-C), 752 (P-C); ¹H NMR: (CDCl₃, 400 MHz), δ 10.95 (s, 1H, OH), 8.15-7.70 (m, 6H, Ar-H), 7.41-7.38 (m, 2H, Ar-H), 6.88 (d, $J = 12.0$ Hz, 1H, Ar-H), 4.97 (d, $J = 12.0$ Hz, 1H, P-CH), 4.71 (s, 1H, CH-NH), 3.72-3.64 (m, 6H, O-CH₃) 2.62 (s, 3H, CH₃) ppm; ¹³C NMR (CDCl₃, 100 MHz), δ 155.80, 146.90, 143.25, 138.95, 136.23, 131.04 (d, $J = 40.0$ Hz), 129.69, 128.74 (t, $J_1 = 5.0$ Hz, $J_2 = 12.0$ Hz), 125.17, 121.66, 69.89, (d, $J = 161.0$ Hz), 63.23 (t, $J_1 = 7.0$ Hz, $J_2 = 8.0$ Hz), 33.60 ppm; ³¹P NMR (CDCl₃, 161.9 MHz) δ 20.36 ppm; LCMS (ESI): m/z calculated for C₁₉H₂₁N₂O₄P: [M+H]⁺ 373.4563, found 373.4560.

Synthesis and antimicrobial activity of novel α -aminophosphonates

Dimethyl ((2-hydroxynaphthalen-1-yl)((4-methoxyphenyl)amino)methyl)phosphonate (4g): Yellow solid, Yield: 95%, mp: 138-139 °C. FTIR (neat) ($\nu_{\max}/\text{cm}^{-1}$): 3385 (NH), 1220 (P=O), 1039 (P-O-C), 794 (P-C); ^1H NMR: (CDCl_3 , 400 MHz), δ 11.05 (s, 1H, OH), 9.03-8.57 (m, 6H, Ar-H), 7.41 (d, $J = 8.0$ Hz, 2H, Ar-H), 6.89 (d, $J = 8.0$ Hz, 2H, Ar-H), 4.98 (d, $J = 8.0$ Hz, 1H, P-CH), 4.4 (s, 1H, CH-NH) 3.80 (s, 3H, -OCH₃), 3.72-3.64 (m, 6H, O-CH₃) ppm; ^{13}C NMR (CDCl_3 , 100 MHz), δ 159.58, 158.19, 151.75 (d, $J = 21.0$ Hz), 128.76 (t, $J_1 = 71.0$ Hz, $J_2 = 6.0$ Hz) 127.48, 126.56 (d, $J = 24.0$ Hz), 115.40, 113.87, 114.47, 112.73, 112.11, 108.86, 70.16 (d, $J = 160.0$ Hz), 69.36, 55.27, 53.89 (d, $J = 7.0$ Hz) 53.62 (d, $J = 7.0$ Hz) ppm; ^{31}P NMR (CDCl_3 , 161.9 MHz) δ 20.77 ppm; LCMS (ESI): m/z calculated for $\text{C}_{20}\text{H}_{22}\text{NO}_5\text{P}$: $[\text{M}+\text{H}]^+$ 388.3242, found 388.3238.

Dimethyl ((2-hydroxynaphthalen-1-yl)(pyrimidin-2-ylamino)methyl)phosphonate (4h): Orange solid, Yield: 95%, mp: 138-139 °C. FTIR (neat) ($\nu_{\max}/\text{cm}^{-1}$): 3385 (NH), 1240 (P=O), 1039 (P-O-C), 791 (P-C); ^1H NMR: (CDCl_3 , 400 MHz), δ 10.93 (s, 1H, OH), 8.23-7.89 (m, 3H, Ar-H), 7.75 (t, $J_1 = 32.0$ Hz, $J_2 = 28.0$ Hz, 3H, Ar-H), 6.96 (s, 1H, Ar-H), 6.86 (d, $J = 8.0$ Hz, 1H, Ar-H), 6.72 (t, $J_1 = 4.0$ Hz, $J_2 = 8.0$ Hz, 1H, Ar-H), 4.88 (d, $J = 8.0$ Hz, 1H, P-CH), 4.38 (s, 1H, CH-NH), 3.68-3.61 (m, 6H, CH₃) ppm; ^{13}C NMR (CDCl_3 , 100 MHz), δ 160.40, 159.95, 156.20, 154.79, 150.96 (d, $J = 29.0$ Hz), 146.69 (d, $J = 15.0$ Hz), 141.07, 135.99, 129.26, 125.52, 119.84 (d, $J = 7.0$ Hz), 114.60, 106.9 (t, $J_1 = 38.0$ Hz, $J_2 = 5.0$ Hz), 69.41 (d, $J = 160.0$ Hz), 53.05 (d, $J = 7.0$ Hz), 52.67 (d, $J = 7.0$ Hz) ppm; ^{31}P NMR (CDCl_3 , 161.9 MHz) δ 18.99 ppm; LCMS (ESI): m/z calculated for $\text{C}_{17}\text{H}_{18}\text{N}_3\text{O}_4\text{P}$: $[\text{M}+\text{H}]^+$ 360.6483, found 360.6479.

Dimethyl((2-hydroxynaphthalen-1-yl)((5-nitropyridin-2-yl)amino)methyl)phosphonate (4i): Brown solid, Yield: 94%, mp: 138-139 °C. FTIR (neat) ($\nu_{\max}/\text{cm}^{-1}$): 3362 (NH), 1247 (P=O), 1079 (P-O-C), 772 (P-C); ^1H NMR: (CDCl_3 , 400 MHz), δ : 10.77 (s, 1H, OH), 8.03-7.71 (m, 6H, Ar-H), 7.47 - 7.25 (m, 3H, Ar-H), 4.99 (d, $J = 44$ Hz, 1H, P-CH), 4.42 (s, 1H, CH-NH), 3.69-3.66 (m, 6H, O-CH₃) ppm; ^{13}C NMR (CDCl_3 , 100 MHz), δ 160.52, 158.55, 156.68 (d, $J = 9.0$ Hz) 155.96, 152.20, 145.17, 135.74 (d, $J = 2$ Hz), 131.54 (d, $J = 3.0$ Hz) 128.77 (d, $J = 6.0$ Hz), 123.92, 122.23 (d, $J = 4.0$ Hz), 117.83 (d, $J = 26.0$ Hz), 108.85, 108.14, 70.79, 69.99 (d, $J = 160.0$ Hz), 54.21 (d, $J = 7.0$ Hz), 53.74 (d, $J = 8$ Hz) ppm; ^{31}P NMR (CDCl_3 , 161.9 MHz) δ 18.72 ppm; LCMS (ESI): m/z calculated for $\text{C}_{18}\text{H}_{18}\text{N}_3\text{O}_6\text{P}$: $[\text{M}+\text{H}]^+$ 404.2560, found 404.2557.

Dimethyl (((3-chloro-4-fluorophenyl)amino)(2-hydroxynaphthalen-1-yl)methyl)phosphonate (4j): Yellow solid, Yield: 95%, mp: 138-139 °C. FTIR (neat) ($\nu_{\max}/\text{cm}^{-1}$): 3335 (NH), 1226 (P=O), 1033 (P-O-C), 799 (P-C); ^1H NMR: (CDCl_3 , 400 MHz), δ 10.94 (s, 1H, OH), 8.10 (s, 1H, Ar-H), 8.01 (d, $J = 8.0$ Hz, 1H, Ar-H), 7.37-7.13 (m, 4H, Ar-H) 6.60-6.53 (m, 3H, Ar-H), 5.22 (d, $J = 12.0$ Hz, 1H, P-CH), 4.85 (s, 1H, CH-NH), 3.85-3.79 (m, 6H, O-CH₃) ppm; ^{13}C NMR (CDCl_3 , 100 MHz), δ 159.17, 151.86, 146.65 (d, $J = 15.0$ Hz), 133.06 (d, $J = 14.0$ Hz), 132.28, 130.18, 127.51 (d, $J = 14.0$ Hz), 122.57, 119.80, (d, $J = 8.0$ Hz), 108.48, 69.36 (d, $J = 161.0$ Hz), 52.96, (d, $J = 7.0$ Hz), 52.63 (d, $J = 7.0$ Hz) ppm; ^{31}P NMR (CDCl_3 , 161.9 MHz) δ 21.56 ppm; LCMS (ESI): m/z calculated for $\text{C}_{19}\text{H}_{18}\text{ClFNO}_4\text{P}$: $[\text{M}+\text{H}]^+$ 410.0717, found 410.0714.

2.4. Biological Activity Assays

2.4.1. Antibacterial Activity

The *in vitro* antibacterial activity of the title compounds **4a-j** was inspected against both Gram +ve microscopic organisms viz. *Bacillus subtilis* (ATCC 21332), *Staphylococcus aureus* (ATCC 25923) and Gram-ve microorganisms viz. *Escherichia coli* (ATCC 25922), *Pseudomonas aeruginosa* (ATCC 27853) by using disc diffusion method at three concentrations (100, 50, 25 ppm)⁶⁵ with reference to Streptomycin which was used as a standard. 200 μl of active culture of unique microorganism was poured on sterile agar plates and spread frivolously over through sterile glass rod. The discs had been measured 6 mm diameter and have been arranged from Whatman No.1 filter paper and sterilized by autoclaving. The sterile discs have been soaked in check samples title compounds **4a-**

j which were dissolved in DMSO act as negative control, the plates incubated at 37°C in incubator for 24 hours and the zone of inhibition was measured (Diameter in mm).

2.4.2. Antifungal Activity

The title compounds **4a-j** were taken for the evaluation of antifungal activity against three fungal strains *viz.* *Candida albicans* (ATCC 18804), *Aspergillus niger* (ATCC 16888) and *Rhizopus oryzae* (ATCC 200756) at different concentrations (100, 50, 25 ppm) with reference to Fluconazole which was used as a standard. The Antifungal activity was done by using paper disc diffusion method⁶⁶. At first, the Potato Dextrose Agar media was poured in petri plates and permitted for solidification followed by 150 µl of fungal inoculums was dispersed equably on the surface of the agar medium with sterile glass spreader. Sterile paper plates were splashed in 25 mL of titled compounds and set on agar media for their antifungal activity. The inoculated plates were incubated at 37 °C for 48-72 hours and the zone of inhibition was measured in mm as diameter.

2.4.3. Determination of Antimicrobial Activity (MIC)

All the newly synthesized α -aminophosphonates **4a-j** were tested for their *in vitro* antimicrobial activity against bacterial strains (*Bacillus subtilis*, *Staphylococcus aureus*, *Escherichia coli* and *Pseudomonas aeruginosa*) and fungal strains (*Candida albicans*, *Aspergillus niger* and *Rhizopus oryzae*) by disc diffusion method⁶⁷. Streptomycin and Voriconazole were used as standard control for bacteria and fungi respectively. Preliminary screening of the title compounds **4a-j** and standard drugs were performed at fixed concentrations of 500 µg/mL. Inhibition was recorded by measuring the diameter of the inhibition zone at the end of 24 h for bacteria and 72 h for fungi. Each experiment was repeated twice. Based on the results of zone of inhibition, the minimum inhibitory concentration (MIC) of compounds **4a-j** against all bacterial and fungal strains was determined by liquid dilution method. Stock solutions of tested compounds with 200, 100, 50, 25, 12.5 and 6.25 µg/mL concentrations were prepared with DMSO solvent. The solutions of standard drugs, Streptomycin and Voriconazole were prepared in the same concentrations. Inoculums of the bacterial and fungal culture were also prepared. To a series of tubes each containing 1 mL of title compound solution with different concentrations and 0.2 mL of the inoculums was added. Further 3.8 mL of the sterile water was added to each of the test tubes. These test tubes were incubated for 24 h at 37°C and observed for the presence of turbidity. This method was repeated by changing title compounds with standard drugs Streptomycin and Voriconazole for comparison. The minimum inhibitory concentration at which no growth observed was taken as the MIC values (Table 6). The comparison of the MICs (in µg/mL) of potent compounds and standard drugs against tested strains are presented in Table 6.

2.5. In-silico Molecular Docking and ADMET Studies

2.5.1. Protein Structure Preparation and Re-docking

The X-ray crystal structures (PDB codes 2VF5 (*Escherichia coli*) and 2POC (*Candida albicans*) were retrieved from the Protein Data Bank (PDB). After removing all water molecules and heteroatoms from the complexes, YASARA software was used to minimize protein stereochemical clashes. Subsequently, the ligand-binding domains of the receptor structures were selected using a grid-based approach facilitated by the DoGSiteScorer program. A potential docking site was modeled using the Autoligand module in AutoDock Tools, using estimates of druggable pocket volume, surface properties and ligand coverage. Grid parameters were defined using the AutoGrid module with center coordinates set to 29.7082 × 15.8539 × -3.2967 Å³ and 20 × 20 × 20 Å³ for 2VF5; 69.4486 × -4.9492 × 50.7769 Å³ and 20 × 20 × 20 Å³ size for 2POC, all points spaced by 0.371 Å. Consequently, all flexible residues are strategically placed to optimize ligand interactions within this grid. Finally, the .pdb files were converted to AutoDock.pdbqt files by adding Gasteiger charges using PyRx software.

Next, a re-docking procedure was performed using the native ligands of the 2VF5 and 2POC structures, namely GLP (2-amino-2-deoxy-6-*O*-phosphono- α -D-glucopyranose) and UD1 (Uridine-Diphosphate-*N*-Acetylglucosamine) with corresponding PDB codes. This phase aims to standardize the docking protocol. The protonation state of the native ligands was adjusted to pH 7.4

Synthesis and antimicrobial activity of novel α -aminophosphonates

and converted to the AutoDock ligand format using Open Babel software. Subsequently, ligands were subjected to docking against the pocket grid using an empirical free energy scoring function and Lamarckian genetic algorithms *via* AutoDock Vina facilitated by the PyRx virtual screening program. Local binding searches for ligand interaction were performed using the Solis–Wets algorithm, with 10 integral runs for each ligand.

2.5.2. Virtual Screening and Molecular Docking

Virtual screening and molecular docking play key roles in contemporary structure-based drug discovery. Initially, to optimize the ligand interaction stability in the complex, their protonation states were adjusted to the neutral point (pH: 7.4) by introducing polar hydrogens. Subsequently, refinement of ligand stereochemical clashes was performed by lead optimization using the conjugate gradient minimization algorithm in the OpenBabel module. These optimized leads were saved as a dataset for further docking assessments. Following the standard docking methodology mentioned above, the lead library from the initial screening step was subjected to virtual screening against the ligand-binding domain. This process involves three replicates using a flexible docking approach that considers flexible pocket residues. Complexes were saved based on the lowest ΔG binding energy conformations obtained from these compounds. For the analysis of potential protein-ligand interactions, the molecular interaction profiler program was used and the results were visualized using PyMOL software.

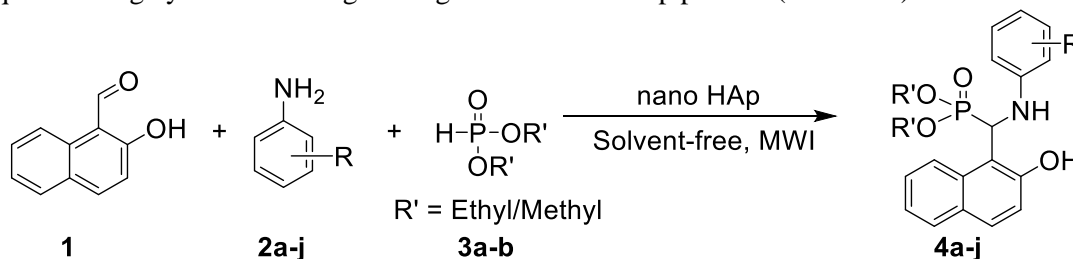
2.5.3. Assessment of Drug-likeness and ADMET Properties

Qualitative evaluation of molecule drug-likeness was performed using the QED program integrated in RDKit v2021.03.4. This estimate is based on eight commonly considered molecular properties including molecular weight (MW), hydrogen bond acceptors (HBAs), hydrogen bond donors (HBDs), molecular polar surface area (PSA), octanol-water partition coefficient (ALOGP), rotatable bonds (ROTBS), aroma rings (AROMs) and structured alerts (ALERTS). To estimate the pharmacokinetic ADME (absorption, distribution, metabolism and excretion) and toxicity profiles, the reliable SwissADME tool was used <http://swissadme.ch/>. This comprehensive analysis allows us to gain insights into the lead-like properties of compounds and their compatibility with positive controls.

3. Results and Discussion

3.1. Chemistry

The goal of this work was setting up synthetic protocols for the obtainment of dendrimeric vectors. Here we developed a simple method for the synthesis of dialkyl ((2-hydroxynaphthalen-1-yl)((substituted phenyl)amino)phosphonate derivatives **4a-j**. It involves the reaction mixture of 2-hydroxy-1-naphthaldehyde (**1**), various aromatic amines (**2a-e**) and dialkyl phosphites (**3a-b**) using catalytic action of HAp NPs under MWI and solvent-free conditions. The target products were acquired in high yields following a straightforward work-up process (Scheme 1).



Scheme 1. Synthesis of dialkyl ((2-hydroxynaphthalen-1-yl)((substituted phenyl)amino)methyl) phosphonate derivatives **4a-j**

In order to optimize the experimental conditions, a model reaction has been carried out for the production of diethyl ((2-hydroxynaphthalen-1-yl)((6-methylpyridin-2-yl)amino) methyl) phosphonate

(**4a**) by the reaction of 2-hydroxy-1-naphthaldehyde (**1**), 2-amino-6-methyl pyridine (**2a**) and diethyl phosphite (**3**). At the outset, the reaction under catalyst-free conditions with conventional heating results in very low yields even after 24 hrs (Table 1, entry 1). Later we run the reaction with various catalysts (Table 1, entries 2-17). Among all the catalysts, HAp NPs worked effectively and provided good product yield of the desired compound (**4a**) (Table 1, entry 17).

Table 1. Optimization of reaction with respect to different catalysts required for synthesis of the compound (**4a**)^a

Entry	Catalyst (10 mol %)	Time (hrs)	Temperature (°C)	Product Yield (%) ^b
1	Catalyst free	8	90	30
2	AlCl ₃	12	80	65
3	ZrOCl ₂ ·8H ₂ O	10	80	68
4	InF ₃	14	100	75
5	ZnBr ₂	16	50	69
6	ZnCl ₂	10	75	60
7	ZnO	15	85	70
8	ZnCl ₂ -SiO ₂	6	95	70
9	MnCl ₂ ·4H ₂ O	8	100	68
10	Yb(OAc) ₃ ·H ₂ O	4	95	76
11	CuBr	12	76	78
12	K-10	9	65	64
13	Al ₂ O ₃	10	55	76
14	NiCl ₂ ·6H ₂ O	8	75	76
15	Amberlyst-15	12	70	77
16	TiO ₂ -SiO ₂	6	80	80
17	HAp NPs	0.5	35	90

^aReaction conditions: 2-hydroxy-1-naphthaldehyde (**1**), 2-amino-6-methyl pyridine (**2a**), diethyl phosphite (**3a**) by using different catalysts along with HAp NPs; ^bIsolated yields.

Table 2. Solvent effect for the synthesis of **4a** in the presence of HAp NPs^a

Entry	Solvent	Time (hrs)	Temperature (°C)	Yield (%) ^b
1	THF	10	60	60
2	Toluene	10	100	70
3	Dioxane	10	60	60
4	DCM	10	50	79
5	Ethanol	6	60	83
6	Methanol	6	50	82
7	Ethylene glycol	2	90	83
8	Glycerol	2	100	87
9	Solvent-free	0.5	35	90

^aReaction conditions: 2-hydroxy-1-naphthaldehyde (**1**), 2-amino-6-methyl pyridine (**2a**), diethyl phosphite (**3a**) by using HAp NPs as catalyst and various solvents. ^bIsolated yield.

Following this, we investigated the impact of various non-polar solvents, including THF, toluene, dioxane and DCM (Table 2, Entries 1-4), as well as polar solvents such as ethanol, methanol, ethylene glycol and glycerol (Table 2, Entries 5-8), alongside without the use of solvent on the reaction using HAp NPs as a catalyst. Toluene, THF, and Dioxane got significantly low product yields, while ethylene glycol and glycerol provided reasonable yields. However, the most favorable

Synthesis and antimicrobial activity of novel α -aminophosphonates

outcomes were achieved when the reaction was conducted without solvent in the presence of HAp NPs catalyst at room temperature. Remarkably, in solvent-free conditions. Under these circumstances, yields were enhanced from 60% to 90% and the reaction time was reduced from hours to minutes (Table 2, Entry 9).

To optimize the catalyst quantity needed under solvent-free conditions with HAp NPs at room temperature, we tested varying amounts: 1, 2.5, 5, 7.5, 10 and 15 mol% (Table 3, Entries 1-6) for 30 minutes. The highest product yield of 94% was achieved using 10 mol% of the catalyst within a 30-minute reaction time. Increasing the catalyst quantity beyond 10 mol% did not enhance the reaction rate or product yields.

Table 3. Optimization of the quantity of the catalyst required the synthesis of compound **4a** at room temperature

Entry	Catalyst loaded (mol%)	Time (min)	Yield (%) ^b
1	1	30	73
2	2.5	30	85
3	5	30	89
4	7.5	30	90
5	10	30	94
6	15	30	92
7	20	30	92

^aReaction conditions: 2-hydroxy-1-naphthaldehyde (**1**), 2-amino-6-methyl pyridine (**2a**), diethyl phosphite (**3a**) by using different mol (%) of catalyst; ^bIsolated yield.

The Kabachnik-Fields reaction is known to be temperature-sensitive. While high levels of microwave energy can accelerate the reaction rate, they also trigger side reactions and lead to the decomposition of formed products into corresponding aldehydes and amines. Hence, it was observed that subjecting the reaction substrates to 200 W of microwave radiation for 6 minutes is adequate to complete the reaction. For exploring energy preferences, the reaction was conducted using conventional and microwave heating at 200 W. Determination of the required catalyst quantity for the reaction at 200 W for 6 minutes revealed that 7.5 mol% of the catalyst was optimal for achieving maximum product yield (94%) under these conditions (Table 4). Furthermore, to ascertain the suitable microwave power for the reaction, experiments were carried out at 100, 200, 300, 350, 400, 450, and 500 W with 15 mol% of the catalyst. The results indicated that 200 W microwave power is adequate to yield satisfactory outcomes (Table 4, Entry 7).

Table 4. Effect of microwaves power (W) and amount of the catalyst on the yield of the product (**4a**)^a

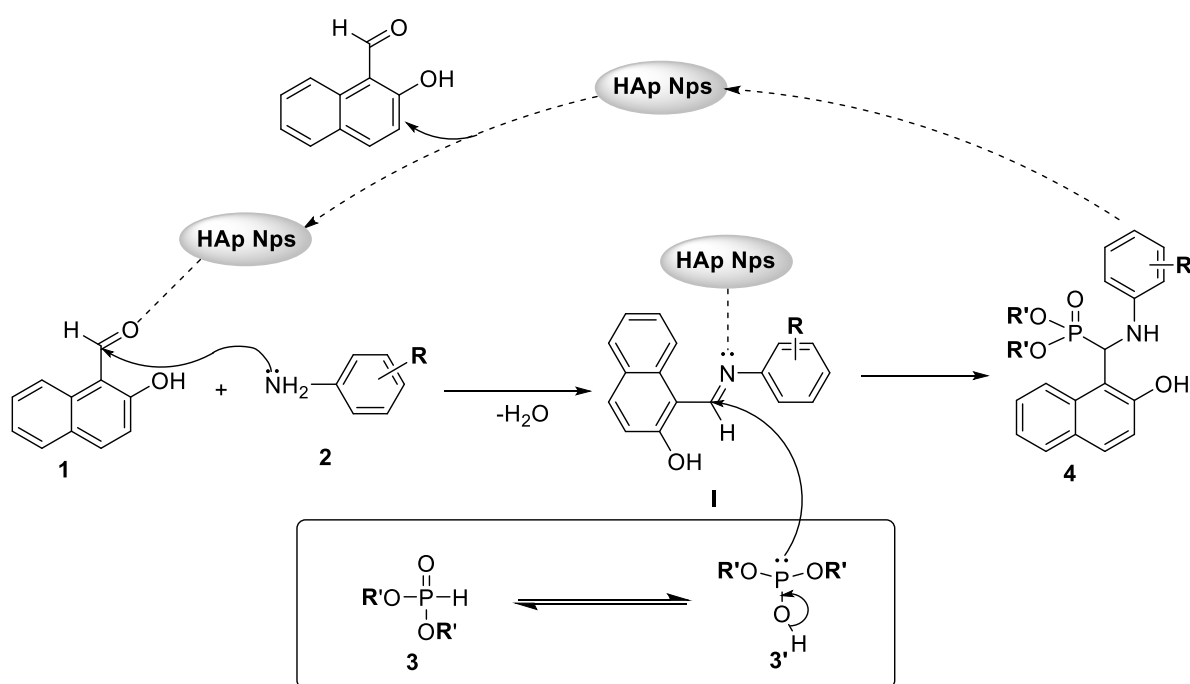
Entry	Catalyst (mol %)	MWI (W)	Time (min)	Yield (%) ^b
1	1	100	15	90
2	2.5	100	15	92
3	5	100	10	92
4	7.5	200	10	96
5	10	200	6	94
6	15	200	6	92
7	20	200	6	92

^aReaction conditions: 2-hydroxy-1-naphthaldehyde (**1**), 2-amino-6-methyl pyridine (**2a**), diethyl phosphite (**3a**) by using different mol (%) of catalyst under MWI conditions; ^bIsolated yield.

The method's generality and applicability were thoroughly investigated. Keeping the reaction conditions consistent, we advanced to explore its effectiveness across various reactions. Several aryl amines (**2a-e**) were reacted with 2-hydroxy-1-naphthaldehyde (**1**), diethyl and dimethyl phosphites (**3a-b**) and the outcomes are summarized in Table S1. The experimental findings demonstrated the proficiency of the catalyst across a range of substituted amines. These results affirm that HAp NPs effectively catalyzes the synthesis of α -aminophosphonates under both conventional and microwave-assisted methods (Scheme 1). The microwave technique offers notable advantages over the

conventional method, including excellent product yields, shorter reaction times and reduced catalyst quantities.

The suggested mechanism (Scheme 2) for the formation of α -aminophosphonates **4a-j** involving the use of HAp NPs as a catalyst involves several steps. Initially, HAp NPs increases the electrophilicity of the carbonyl carbon (**1**), facilitating the nucleophilic attack of an amine (**2**) onto the electrophilic carbonyl carbon of the aldehyde. Simultaneously, water is eliminated, leading to the formation of an imine intermediate (**I**). Subsequently, the nucleophilic dialkyl phosphite (**3**) attacks the electrophilic carbon of the imine intermediate (**I**), resulting in the formation of a C–P bond and ultimately yielding the desired α -aminophosphonate (**4**).



Scheme 2. Mechanistic pathway for the synthesis of α -aminophosphonates **4a-j** by Kabachnik-Field's reaction using HAp NPs as catalyst

3.2. Biological Activity

3.2.1. *In vitro* Antibacterial Activity

The antibacterial activity of the newly synthesized dialkyl ((2-hydroxynaphthalen-1-yl)((substituted phenyl)amino)phosphonate derivatives **4a-j** was inspected by screening them against Gram +ve (*Staphylococcus aureus* and *Bacillus subtilis*) and Gram –ve (*Pseudomonas aeruginosa* and *Escherichia coli*) bacteria using disc diffusion method⁶⁵. The compounds **4h**, **4i**, **4j** and **4e** showed good activity when compared to that of the standard Streptomycin against tested bacteria. A few of the compounds exhibited moderate inhibitory activity. The zones of restraint of diverse compounds were presented in Table 5. The results displayed that the most of the compounds showed significant activities against used bacterial cultures.

Synthesis and antimicrobial activity of novel α -aminophosphonates**Table 5.** Antibacterial activity of α -aminophosphonates **4a-j**

S. No.	Compounds	Gram (+)		Gram (-)	
		<i>Bacillus Subtilis</i> (ZOI in mm)	<i>Streptococcus Aureus</i> (ZOI in mm)	<i>Escherichia Coli</i> (ZOI in mm)	<i>Pseudomonas aeruginosa</i> (ZOI in mm)
1	4a	4.4±0.6	2.6±0.4	2.5±0.4	1.4±0.3
2	4b	3.6±0.4	2.4±0.2	1.6±0.4	0.9±0.6
3	4c	2.0±0.6	0.6±0.3	1.6±0.1	1.2±0.9
4	4d	8.4±0.3	6.8±0.2	5.4±0.2	4.1±0.4
5	4e	7.6±0.3	5.2±0.1	4.6±0.3	3.4±0.6
6	4f	2.6±0.4	1.6±0.2	1.3±0.2	1.9±0.2
7	4g	0.8±0.2	1.3±0.8	1.2±0.2	1.2±0.3
8	4h	6.0±0.2	4.6±0.5	1.8±0.2	1.6±0.4
9	4i	7.6±0.4	4.8±0.2	3.2±0.2	3.8±0.2
10	4j	6.8±0.2	4.2±0.8	3.0±0.3	2.6±0.4
11	Streptomycin	6.2±0.4	4.6±0.2	3.2±0.2	2.8±0.6

ZOI: zone of inhibition in mm

3.2.2. *In vitro* Antifungal Activity Assays

The antifungal activity of the title compounds **4a-j** was inspected by screening them against *Aspergillus niger*, *Candida albicans* and *Rhizopus oryzae* using disc diffusion method⁶⁶. Among all the title compounds **4d**, **4e**, **4i** and **4j** showed excellent antifungal activity when compared to that of the standard. The findings are displayed in the Table 6.

Table 6. Antifungal activity of α -aminophosphonates (**4a-j**).

S. No.	Compounds	<i>Aspergillus niger</i> (ZOI in mm)	<i>Rhizopus oryzae</i> (ZOI in mm)	<i>Candida albicans</i> (ZOI in mm)
1	4a	0.6±0.4	0.2±0.6	0.3±0.2
2	4b	1.2±0.4	1.2±0.4	0.2±0.3
3	4c	1.0±0.6	1.0±0.6	0.4±0.8
4	4d	3.2±0.4	2.8±0.4	2.6±0.3
5	4e	3.6±0.1	2.4±0.3	2.3±0.1
6	4f	1.0±0.4	0.4±0.6	1.2±0.4
7	4g	1.4±0.8	0.2±0.4	1.8±0.3
8	4h	1.6±0.2	1.6±0.2	1.4±0.2
9	4i	2.8±0.3	1.8±0.6	1.8±0.4
10	4j	2.7±0.4	1.6±0.8	1.8±0.1
11	Voriconazole	2.4±0.2	1.6±0.4	1.8±0.8

ZOI: zone of inhibition in mm

All the synthesized compounds were screened for their *in vitro* antibacterial activity against both Gram +ve (*Staphylococcus aureus* & *Bacillus subtilis*) and Gram -ve (*Pseudomonas aeruginosa* & *Escherichia coli*) bacteria and MIC values of all compounds was also determined⁶⁷, which is defined as the lowest concentration of inhibitor at which bacterial growth was not visually apparent. Investigation on antibacterial screening data showed some of the compounds were active against four human pathogenic bacteria. Compounds **4d**, **4e**, **4i** and **4j** showed good activity against *Staphylococcus aureus* and *Escherichia coli* when compared to the standard Streptomycin while the remaining compounds showed moderate inhibitory activity (Table 8).

In vitro antifungal activity of the produced compounds against *Candida albicans*, *Aspergillus niger* and *Rhizopus oryzae* was evaluated. The results revealed that the title compounds exhibited variable degree of inhibition against the tested fungi. Out of all the title compounds **4d**, **4e**, **4i** and **4j** exhibited excellent antifungal activity when compared than that of the standard drug Voriconazole.

The anti-fungal activity of the remaining compounds was found to be good when compared to that of the standard drug Voriconazole (Table 7).

Table 7. Minimum Inhibitory Concentration (MIC) values of α -aminophosphonates **4a-j**

		Minimum inhibitory concentration (MIC) in $\mu\text{g/mL}$						
S. No.	Tested Samples	Bacterial Strains				Fungal Strains		
		<i>Bacillus subtilis</i>	<i>Streptococcus aureus</i>	<i>Escherichia coli</i>	<i>Pseudomonas aeruginosa</i>	<i>Aspergillus niger</i>	<i>Rhizopus oryzae</i>	<i>Candida albicans</i>
1	4a	200	100	50	250	125	500	250
2	4b	50	50	100	100	250	125	250
3	4c	100	200	100	200	125	250	500
4	4d	6.25	6.25	6.25	6.25	31.25	31.25	31.25
5	4e	6.25	6.25	6.25	6.25	64.50	64.50	64.50
6	4f	100	100	200	200	250	500	125
7	4g	100	200	200	100	250	250	250
8	4h	50	200	100	50	500	250	250
9	4i	6.25	6.25	6.25	6.25	31.25	31.25	31.25
10	4j	12.5	12.5	12.5	6.25	64.50	64.50	64.50
11	Streptomycin	6.25	6.25	6.25	6.25	-	-	-
12	Voriconazole	-	-	-	-	31.25	31.25	31.25

3.2.3. Re-docking

The ligand GLP, located in the isomerase domain of 2VF5, exhibited significant properties: volume 584.64 \AA^2 , surface area 569.23 \AA^2 , depth 17.09 \AA and drug score 0.78. In contrast, the ligand UD1, located in the surface isomerase domain (inhibitor binding site) of 2POC, exhibited remarkable properties: volume 368.9 \AA^2 , surface area 404.26 \AA^2 , depth 19.09 \AA , and drug score 0.77. Consequently, a finely tuned grid with high efficiency was generated by the autoligand and autogrid modules, considering the anticipated binding site granularity and druggability for the two receptors. Subsequently, a re-docking procedure was performed for the ligands GLP and UD1 in the active site using AutoDock Vina in the PyRx program⁶⁸.

In the re-docking conformation, 2-amino-2-deoxy-6-*O*-phosphono- α -D-glucopyranose (GLP) forms hydrogen bonds with Thr302, Ser303, Ser347, Gln348, Ser349, Glu488 and Ala602. A ΔG binding energy of -6.3 kcal/mol. Structural superposition of the two conformations revealed a root-mean-square deviation (RMSD) of 1.0 \AA (Figure 1a and 1b). Similarly, in the re-docking conformation, Uridine-Diphosphate-*N*-Acetylglucosamine (UD1) forms hydrogen bonds with Gly384, Thr487, Gly490 and His492, resulting in a ΔG binding energy of -6.1 kcal/mol. interestingly, the phosphate group of UD1 forms salt bridges with Arg372 and His492. Structural superposition of the two conformations revealed a root-mean-square deviation (RMSD) of 1.0 \AA (Figure 2a and 2b). These findings underscore the effectiveness of a standardized docking protocol, with ligand binding patterns indicating interactions with active site residues and additional bonds that stabilize the receptor domain, thereby facilitating inhibition of GlcN-6-P synthase. Consequently, inhibitors may block receptor conformation at flexible points, thereby reducing initiation of hexosamine metabolic pathways supported by GlcN-6-P synthase activation.

3.2.4. Analysis of Protein-Ligand Interaction Profiles and Molecular Docking

3.2.4.1 Mode of Binding of Ligands with 2VF5

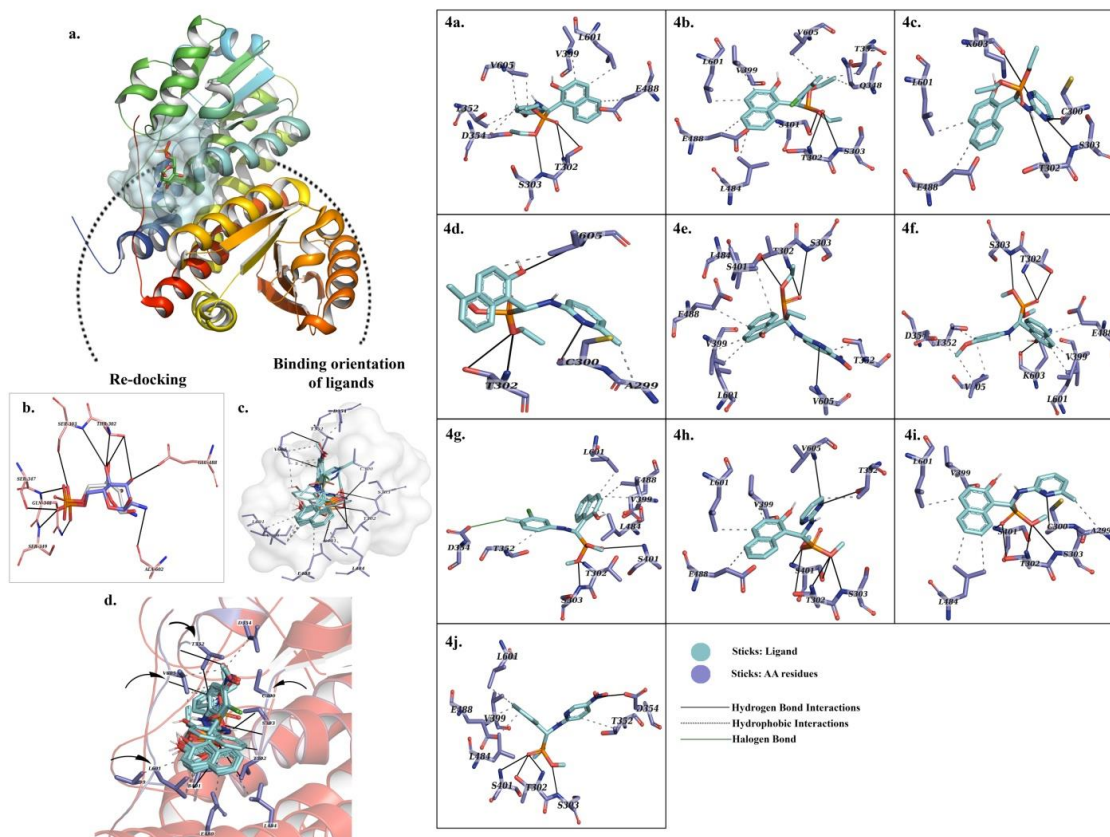


Figure 1. Analysis of protein-ligand interaction profiles. **a.** Structure of the 2VF5 complex: The surface is represented in cyan, indicating the ligand binding domain. **b.** Re-docking conformation of the native ligand (GPL): The native conformation is depicted in white sticks, while the re-docking conformation is shown in blue sticks. **c.** Binding orientation of all lead compounds within the GPL binding cavity: The active site is represented by the white surface, with ligands depicted in cyan sticks and amino acid residues shown in blue sticks. **d.** Conformational changes observed in protein loops and helices following ligand binding are indicated with arrows.

Thorough virtual screening and docking processes revealed that the novel compounds ΔG binding free energy ranged from -7.1 to -8 kcal/mol. For the novel compounds **4a-j** with 2VF5, as delineated in Table 8. Remarkably, these newly discovered leads displayed typical binding patterns within the domain, akin to those observed with the positive control (GPL), and exhibited favorable binding affinities (Figure 1c). All these leads showcased binding to the GPL binding domain of the receptor structure, establishing potential hydrogen bonds with flexible amino acid residues such as Cys300, Thr302, Ser303, Ser401, Lys603, Val605, Thr352, and Asp354 (Table 8 and Figure 1).

Table 8. Protein-ligand interaction profiles of novel compounds with 2VF5

Ligands	ΔG binding kcal/mol	Hydrogen Bond Interactions			Hydrophobic Interactions		Halogen bonds		
		AA Residues	Distance	Angle (Å)	AA Residues	Distance	AA Residues	Distance	Angle (Å)
4a	-7.1				Thr352	3.82			
					Asp354	3.89			
		Thr302	2.93	147.63	Val399	3.94			
		Thr302	2.95	106.52	Glu488	3.76	-	-	-
		Ser303	2.82	164.24	Leu601	3.1			
					Val605	3.75			
					Val605	3.51			
4b	-7.4				Gln348	3.66			
					Thr352	3.87			
		Thr302	3.07	126.16	Val399	3.94			
		Ser303	2.87	161.75	Leu484	3.38	-	-	-
		Ser401	2.79	109.74	Glu488	3.74			
					Leu601	3.2			
					Val605	3.88			
4c	-7.4	Cys300	2.53	118.93					
		Thr302	2.85	144.66	Glu488	3.72			
		Ser303	2.3	157.31	Leu601	3.4	-	-	-
		Lys603	3.37	129.11					
4d	-7.2	Cys300	2.66	110.51					
		Thr302	2.52	152.9	Ala299	3.62			
		Thr302	3.39	111.15	Val605	3.5	-	-	-
		Val605	3.44	106.03					
4e	-7.4	Thr302	3.16	129.85	Thr352	3.13			
		Ser303	3.11	165.86	Val399	3.9			
		Ser401	2.95	106.89	Leu484	3.98	-	-	-
		Val605	2.85	162.66	Glu488	3.77			
					Leu601	3.28			
4f	-7.2				Thr352	3.2			
					Asp354	3.69			
		Thr302	2.99	147.63	Val399	3.91			
		Thr302	2.97	106.47	Glu488	3.7	-	-	-
		Ser303	2.62	156.07	Leu601	3.12			
		Lys603	2.55	123.47	Val605	3.56			
4g	-7.4				Val605	3.51			
					Thr352	3.82			
		Thr302	3.1	123.15	Val399	3.96			
		Ser303	2.76	156.49	Leu484	3.41	Asp354	3.88	155.93
		Ser401	3.34	121.98	Glu488	3.9			
4h	-7.1				Leu601	3.18			
		Thr302	3.61	100.62					
		Thr302	3.13	117.96	Thr352	3.24			
		Ser303	2.68	139.07	Val399	4			
		Thr352	2.65	127.13	Glu488	3.79	-	-	-
		Ser401	2.99	118.07	Leu601	3.36			
		Ser401	3.51	119.47					
Val605	2.95	162.78							
4i	-8	Cys300	2.36	137.2	Ala299	3.93			
		Thr302	2.62	105.16	Val399	3.85	-	-	-

Synthesis and antimicrobial activity of novel α -aminophosphonates

		Thr302	2.93	119.26	Leu484	3.48			
		Ser303	3	127.6	Leu484	3.65			
		Ser401	2.73	138.96	Leu601	3.42			
		Ser401	2.88	106.02					
4j	-7.4	Thr302	3.19	146.4	Thr352	3.9			
		Thr302	2.92	106.29	Val399	3.92			
		Ser303	2.72	151.89	Leu484	3.36	-	-	-
		Asp354	3.38	112.95	Glu488	3.73			
		Ser401	3.13	132.34	Leu601	3.15			
GPL	-6.3	Thr302	3.31	137.04					
		Thr302	1.93	145.95					
		Thr302	3.26	145.13					
		Ser303	2.96	156.45					
		Ser303	2.63	106.59					
		Ser347	2.03	151.5			-	-	-
		Gln348	1.91	160.5					
		Gln348	2.61	170.2					
		Ser349	2.69	161.02					
		Glu488	2.73	128.15					
		Ala602	2.52	131.29					

Notably, compound **4g** engaged in halogen bond formation with the Asp354 residue (Table 9 and Figure 1). Furthermore, additional hydrophobic interactions were noted with pocket residues such as Ala299, Val399, Gln348, Thr352, Asp354, Val399, Leu484, Glu488, and Leu601 (Table 9). In the GLP binding pathway, hydrogen bonds were specifically formed in the 2VF5 domain region, encompassing flexible hotspot residues with the core moiety of the ligands. Additionally, energetically significant hydrophobic interactions and halogen bonds observed in the complexes played a pivotal role in receptor stabilization and enzyme catalysis, particularly through interactions with side-chain residues such as Asp354⁶¹.

Interestingly, alterations in secondary structure elements, including loop rearrangements and helix deformations, were observed in response to ligand binding (Figure 1d). The conformational changes observed in protein loops and helices following ligand binding underscore the dynamic nature of protein-ligand interactions. These structural changes have a vital role in modulating protein stability and activity⁶⁹⁻⁷¹. Consequently, the presence of additional binding patterns, such as hydrophobic interactions and halogen bonds with ligands, indicates a rigid binding mode, signifying the emergence of a novel hotspot in the receptor domain cleft that enhances inhibitory stability. This underscores the novelty of the observed interactions, significantly contributing to complex stability and increasing the effectiveness of GlcN-6-P synthase inhibition.

3.2.4.2 Binding Mode of Ligands with 2POC

Potential virtual screening and docking procedures unveiled ΔG binding free energies ranging from -5.9 to -6.6 kcal/mol for novel compounds (**4a-j**) with 2POC, as outlined in Table 10. Remarkably, these newly discovered leads exhibited distinct binding patterns within the domain, reminiscent of the behavior observed with the positive control (UD1) (Figure 2c).

All of these compounds bind to the inhibitor binding domain of the receptor structure and form potential hydrogen bonds with flexible amino acid residues such as Arg372, Gly383, Gly384, Trp388, Ser484, Thr487, His488, and His492 (Table 9 and Figure 2). Additionally, limited hydrophobic interactions were observed with pocket residues including Arg485 and Val479 (Table 10). Interestingly, alterations in secondary structure elements, including loop rearrangements and helix deformations, were observed in response to ligand binding (Figure 2d). The conformational changes observed in protein loops and helices following ligand binding underscore the dynamic nature of protein-ligand interactions. These structural changes play a vital role in modulating protein stability and activity⁶⁵⁻⁶⁷. In the UD1 binding pathway in the 2POC domain region, limited hydrogen bonds

involving flexible hotspot residues with the core of the ligands are exclusively formed. When there is a native ligand present, these significant binding patterns are essential for both enzyme catalysis and receptor stabilization when a native ligand is present in the isomerase domain. This emphasizes the novelty of the observed interactions, significantly contributing to complex stability and increasing the effectiveness of GlcN-6-P synthase inhibition.

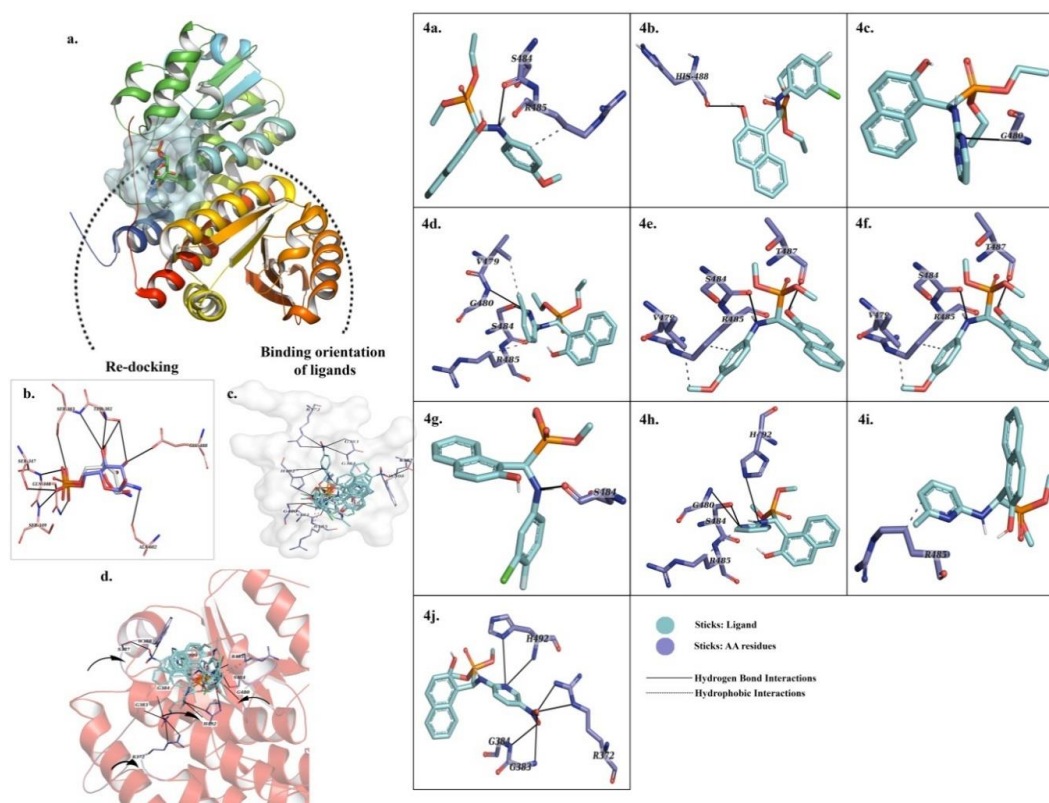


Figure 2. Analysis of protein-ligand interaction profiles. **a.** Structure of the 2POC complex: The surface is represented in cyan, indicating the ligand binding domain. **b.** Re-docking conformation of the native ligand (UD1): The native conformation is depicted in white sticks, while the re-docking conformation is shown in blue sticks. **c.** Binding orientation of all lead compounds within the UD1 binding cavity: The active site is represented by the white surface, with ligands depicted in cyan sticks and amino acid residues shown in blue sticks. **d.** Conformational changes observed in protein loops and helices following ligand binding are indicated with arrows.

Table 9. Protein-ligand interaction profiles of novel compounds with 2POC.

Ligands	ΔG binding kcal/mol	Hydrogen Bond Interactions			Hydrophobic Interactions	
		AA Residues	Distance	Angle (Å)	AA Residues	Distance
4a	-6.2	Ser484	2.29	126.72	Arg485	3.66
4b	-6.3	His488	2.9	111.5	-	-
4c	-6.1	Gly480	3.42	112.06	-	-
4d	-6.3	Gly480	3.51	110.66	Val479	3.75
		Ser484	3.17	114.81	Arg485	3.84
4e	-6.6	Trp388	2.25	141.29	-	-
4f	-6	Ser484	1.95	159.21	Val479	3.8
		Thr487	2.01	138.48	Arg485	3.65
4g	-6.5	Ser484	1.99	2.89	-	-
4h	-6.2	Gly480	3.4	108.83	-	-
		Ser484	2.66	121.79	-	-
		His492	3.54	110.82	-	-
4i	-5.9	-	-	-	Arg485	3.68
4j	-6.6	Arg372	2.75	141.83	-	-
		Arg372	2.15	164.23	-	-
		Gly383	3.23	130.29	-	-
		Gly384	2.22	169.25	-	-
		His492	3.08	109.88	-	-
		His492	2.82	139.5	-	-
UD1	-6.1	Gly384	3.38	108.77	-	-
		Thr487	1.91	166.84	-	-
		Thr487	2.74	133.41	-	-
		Gly490	2.89	129.78	-	-
		Gly490	3.57	108.33	-	-
		His492	2.02	168.77	-	-

3.2.4.3. Pharmacokinetics Properties

Evaluation of drug similarity and physicochemical properties, including pharmacokinetics, of lead compounds was conducted using robust QED, SwissADME, and OSIRIS property programs. As mentioned in Table 10, the potential lead scaffolds adhered to Lipinski's rule of five principles, such as MW (≤ 500 Daltons), HBA (≤ 10), HBD (≤ 5), ALOGP (≤ 5), PSA (≤ 140), and ROTB (≤ 10), respectively. QED scores ranged from 0.2 to 0.6, providing empirical rationale to clarify the molecular properties underlying distribution. This suggests that chemical compounds responsible for pharmacological and biological activity are generally orally active, moderate in size, and possess a degree of lipophilicity.

In terms of ADME observations, seven drug candidates exhibited high levels of gastrointestinal absorption (GIA). None of the compounds demonstrated blood-brain barrier permeability (BBB permeability) activity. All candidates are predicted to be metabolized by different CYP450 gene isoforms, indicating efficient metabolism with high absorption rates, membrane permeability, and low toxicity. Additionally, all candidates comply with the five Lipinski rules.

Overall, our research demonstrates that toxicogenomics, when integrated into the assessment of drug-likeness properties, yielded valuable compounds with low toxic effects and favorable ADME characteristics, suggesting systematic excretion. These findings support the potential suitability of these core compounds as small molecules, particularly inhibitors targeting GlcN-6-P synthase for potential antibacterial and antifungal applications.

Table 10. A quantitative assessment of drug-likeness, RO5 principles and ADMET properties of the lead compounds.

Compound	4a	4b	4c	4d	4e	4f	4g	4h	4i	4j
Drug-likeness predictions										
MW (≤500 Daltons)	415.4	437.8	387.4	400.4	431.4	387.4	409.8	359.3	372.3	403.3
HBA (≤10)	6	5	7	6	8	6	5	7	6	8
HBD (≤5)	2	2	2	2	2	2	2	2	2	2
ALOGP (≤5)	5.931	6.715	4.712	5.626	5.225	5.151	5.935	3.932	4.845	4.445
PSA (≤140)	77.02	67.79	93.57	80.68	123.8 2	77.02	67.79	93.57	80.68	123.8 2
ROTB (≤10)	9	8	8	8	9	7	6	6	6	7
QED	0.454	0.43	0.548	0.503	0.234	0.559	0.529	0.65	0.609	0.286
SwissADME predictions (ADME)										
GI absorption	High	Low	High	High	Low	High	High	High	High	Low
BBB permeant	No	No	No	No	No	No	No	No	No	No
Pgp substrate	Yes	Yes	Yes	No	No	No	No	Yes	Yes	No
CYP1A2 inhibitor	No	No	Yes	Yes	No	No	No	Yes	Yes	Yes
CYP2C19 inhibitor	Yes	Yes	Yes	Yes	Yes	Yes	Yes	Yes	Yes	Yes
CYP2C9 inhibitor	Yes	Yes	Yes	Yes	Yes	Yes	Yes	No	No	Yes
CYP2D6 inhibitor	Yes	Yes	Yes	Yes	Yes	Yes	Yes	Yes	Yes	Yes
CYP3A4 inhibitor	Yes	Yes	Yes	Yes	Yes	Yes	Yes	Yes	Yes	Yes
log Kp (cm/s)	-5.72	-5.33	-6.52	-5.85	-6.45	-6.07	-5.68	-6.87	-6.2	-6.79
Lipinski violations	0	0	0	0	0	0	0	0	0	0

4. Conclusion

We have devised a highly efficient and environmentally friendly method for synthesizing various α -aminophosphonates by employing HAp NPs as a catalyst in a one-pot three-component Kabachnik-Fields reaction, which involves an aldehyde, various aryl amines and dialkyl phosphites. This innovative approach is considered green due to its utilization of an affordable, non-toxic catalyst, solvent-free conditions, straightforward work-up procedure and attainment of high yields. The compounds **4d**, **4e**, **4i** and **4j** exhibited notable activity, as evidenced by studies on ADMET and molecular docking which indicated favorable interactions and promising drug-like properties of the lead molecules. In conclusion, the study indicates that the newly synthesized α -aminophosphonates could emerge as promising lead candidates possessing potent antibacterial and antifungal properties.

Acknowledgements

The author Ms. Sumithra Poreddy acknowledges Virchow Petrochemicals Pvt. Ltd., Hyderabad, Telangana, India for Financial Assistance and also thanks to DST-PURSE 2nd Phase Programme at S.V. University, Tirupati, which is supported by DST, New Delhi, India for providing instrumental analysis.

Supporting Information

Supporting information accompanies this paper on <http://www.acgpubs.org/journal/organic-communications>

ORCID

Sumithra Poreddy: [0009-0004-2558-541X](https://orcid.org/0009-0004-2558-541X)

Mohan Gundluru: [0000-0003-1456-4774](https://orcid.org/0000-0003-1456-4774)

Santhisudha Sarva: [0000-0002-5474-9784](https://orcid.org/0000-0002-5474-9784)

Surendra Pothuraju: [0009-0003-7440-0234](https://orcid.org/0009-0003-7440-0234)

Poojitha Bellala: [0009-0002-6330-6579](https://orcid.org/0009-0002-6330-6579)

Kranthi Kumar Konidala: [0000-0003-2278-8639](https://orcid.org/0000-0003-2278-8639)

Suneetha Yeguvapalli: [0000-0002-3035-7196](https://orcid.org/0000-0002-3035-7196)

Cirandur Suresh Reddy: [0000-0002-9804-9683](https://orcid.org/0000-0002-9804-9683)

References

- [1] Ung, S. P.-M.; Li, C. J. From rocks to bioactive compounds: a journey through the global P(V) organophosphorus industry and its sustainability. *RSC Sustainability*, **2023**, *1*, 11-37.
- [2] Kolodiazhnyi, O. I. Phosphorus compounds of natural origin: Prebiotic, stereochemistry, application. *Symmetry* **2021**, *13*, 889.
- [3] Haiduc, I. Thiophosphorus and related ligands in coordination, organometallic and supramolecular chemistry. A personal account. *J. Organometallic Chem.* **2001**, *623*, 29-42.
- [4] Berlicki, L.; Rudziska, E.; Mlynarza, P.; Kafarski, P. Organophosphorus supramolecular chemistry part 1. Receptors for organophosphorus compounds. *Current Org. Chem.* **2006**, *10*, 2285-2306.
- [5] Kafarski, P.; Mlynarza, P.; Rudziska, E.; Berlicki, L. Organophosphorus supramolecular chemistry part 2. Receptors for organophosphorus compounds. *Current Org. Chem.* **2007**, *11*, 1593-1609.
- [6] Jiao, J.; Li, H.; Xie, W.; Zhao, Y.; Lin, C.; Jiang, J.; Wang, L. Host-guest system of a phosphorylated macrocycle assisting structure determination of oily molecules in single-crystal form. *Chem. Sci.* **2023**, *14*, 11402-11409.
- [7] Karasik, A. K.; Balueva, A. S.; Sinyashin, O. G. An effective strategy of P,N-containing macrocycle design. *Compt. Rendus Chim.* **2010**, *13*, 1151-1167.
- [8] Farkhondeh, T.; Mehrpour, O.; Buhmann, C.; Pourbagher-Shahri, A. M.; Shakibaei, M.; Samarghandian, S. Organophosphorus compounds and MAPK signaling pathways. *Int. J. Mol. Sci.* **2020**, *21*, 4258.
- [9] Gu, X.; Yang, Z.; Zhang, L.; Kunerth, S.; Ralf, F.; Karin, W.; Guse, A. H.; Zhang, L. Synthesis and biological evaluation of novel membrane-permeant cyclic adp-ribose mimics: N¹-[(5''-O-phosphorylethoxy)methyl]-5'-O-phosphorylinosine-5',5''-cyclicpyrophosphate (cIDPRE) and 8-substituted derivatives. *J. Med. Chem.* **2004**, *47*, 5674-5682.
- [10] Xu, L.; Walseth, T. F.; Slama, J. T. Cyclic ADP-ribose analogues containing the methylene bisphosphonate linkage: Effect of pyrophosphate modifications on Ca²⁺ release activity. *J. Med. Chem.* **2005**, *48*, 4177-4181.
- [11] Mucha, A.; Kafarski, P.; Berlicki, L. Remarkable potential of the α -aminophosphonate/phosphinate structural motif in medicinal chemistry. *J. Med. Chem.* **2011**, *54*, 5955-5980.
- [12] Kocsis, D.; Varga, P. R.; Keshwan, R.; Nader, M.; Lengyel, M.; Szabo, P.; Antal, I.; Kanai, K.; Keglevich, G.; Erdo, F. transdermal delivery of α -aminophosphonates as semisolid formulations-an *in vitro-ex vivo* study. *Pharmaceutics* **2023**, *15*, 1464.
- [13] Palica, K.; Deufel, F.; Skagseth, S.; Metzler, G. P. D. S.; Thoma, J.; Rasmussen, A. A.; Valkonen, A.; Sunnerhagen, P.; Leiros, H.-K. S.; Andersson, H.; Erdelyi, M. α -Aminophosphonate inhibitors of metallo- β -lactamases NDM-1 and VIM-2. *RSC Med. Chem.* **2023**, *14*, 2277-2300.
- [14] Wang, Q.; Zhu, M.; Zhu, R.; Lu, L.; Yuan, C.; Xing, S.; Fu, X.; Mei, Y.; Hang, Q. Exploration of α -aminophosphonate N-derivatives as novel, potent and selective inhibitors of protein tyrosine phosphatases. *European J. Med. Chem.* **2012**, *49*, 354-364.
- [15] Tantillo, D. J.; Houk, K. N. Fidelity in Hapten Design: How analogous are phosphonate haptens to the transition states for alkaline hydrolyses of aryl esters? *J. Org. Chem.* **1999**, *64*, 3066-3076.
- [16] Gundluru, M.; Santhisudha Sarva, S.; Sumithra Poreddy, S.; Poojitha, B.; Ashwini, J.; Ethiraj, S.; Cirandur, S. R. Design, synthesis, antibacterial evaluation, and molecular docking studies of

- diethyl((substitutedphenyl)((4-(N-(5-methyl-4,5-dihydroisoxazol-3-yl)sulfamoyl)phenyl)amino) methyl) phosphonates. *Synth. Commun.* **2023**, *53*, 2117-2133.
- [17] Sarva, S.; Dunnutala, R.; Tellamekala, S.; Gundluru, M.; Reddy, C. S. Green Synthesis and antimicrobial activity of substituted diethyl (((5-(ethylthio)-1, 3, 4-thiadiazol-2-yl) amino)(phenyl) methyl) phosphonates. *Synth. Commun.* **2022**, *52*, 268-279.
- [18] Aita, S.; Badavath, V. N.; Gundluru, M.; Sudileti, M.; Reddy, N. B.; Gundala, S.; Zyryanov, G. V.; Chamarti, N. R.; Reddy, C. S. Novel α -Aminophosphonates of imatinib intermediate: synthesis, anticancer activity, human abl tyrosine kinase inhibition, ADME and toxicity prediction. *Bioorg. Chem.* **2021**, *109*, 104718.
- [19] Baren, M. H.; Ibrahim, S. A.; Al-Rooqi, M. M.; Ahmed, S. A.; El-Gamil M. M.; Hekal, H. A. A new class of anticancer activity with computational studies for a novel bioactive aminophosphonates based on pyrazole moiety. *Scien. Rep.* **2023**, *13*, 14680.
- [20] Mohan, G.; Badavath, V. N.; Yasmin S. H.; Murali, S.; Reddy, N. B.; Sravya, G.; Zyryanov, G. V.; Cirandur, S. R. Design, synthesis, cytotoxic evaluation and molecular docking studies of novel thiazolyl α -aminophosphonates. *Res. Chem. Intermed.* **2021**, *47*, 1139-1160.
- [21] Reddy, N. B.; Cherreddy, S. S.; Krishna, B. S. Santhisudha, S.; Sreelakshmi, P.; Nayak, S. K. Reddy, C. S. Cellulose-SO₃H catalyzed synthesis of bis(α -aminophosphonates) and their antioxidant activity, *Org. Commun.* **2017**, *10*, 46-55.
- [22] Sreekanth, T.; Mohan, G.; Santhisudha, S.; Reddy, N. M.; Murali, S.; Rajasekhar, A.; Chippada, A. R.; Reddy, C. S. Meglumine sulfate-catalyzed one-pot green synthesis and antioxidant activity of α -aminophosphonates. *Synth. Commun.* **2019**, *49*, 563-575.
- [23] Kitouni, S.; Chafai, N.; Chafaa, S.; Houas, N.; Ghedjati, S.; Djenane, M. Antioxidant activity of new synthesized imine and its corresponding α -aminophosphonic acid: experimental and theoretical evaluation. *J. Mol. Str.* **2023**, *1281*, 135083.
- [24] Hekal, H. A.; Kassab, R. M.; El Salam, H. A. A.; Shaban, E.; . Atlam, F. M. Synthesis, computational studies, molecular docking, anti-inflammatory and antioxidant activities of α -aminophosphonates incorporating an azo chromophore for polyester printing application. *ChemistrySelect* **2023**, *8*, e202204075.
- [25] Sarfaraz Shaikh, S.; Pratik Dhavan, P.; Pinky Singh, P.; Jasmin Uparkar, J.; Vaidya, S. P.; Jadhav, B. L.; Ramana, M. M. V. Design, synthesis and biological evaluation of novel antipyrene based α -aminophosphonates as anti-alzheimer and anti-inflammatory agent. *J. Biomol. Struct. Dyn.* **2023**, *41*, 386-401.
- [26] Hekal, H. A.; Hammad, O. M.; El-Brollosy, N. R.; Salem, M. M.; Allayeh, A. K. Design, synthesis, docking, and antiviral evaluation of some novel pyrimidinone-based α -aminophosphonates as potent H1N1 and HCoV-229E inhibitors. *Bioorg. Chem.* **2024**, *147*, 107353.
- [27] Hkiri, S.; Mekni-Toujani, M.; Üstün, E.; Hosni, K.; Ghram, A.; Soufiane Touil, S.; Samarat, A.; Semeril, D. Synthesis of novel 1,3,4-oxadiazole-derived α -aminophosphonates/ α -aminophosphonic acids and evaluation of their *in vitro* antiviral activity against the avian coronavirus infectious bronchitis virus. *Pharmaceutics* **2023**, *15*, 114.
- [28] Basha, M. H.; Subramanyam, C.; Malar, C. G. R.; Rao, S. S.; Rao, K. P. Nano TiO₂.SiO₂ catalyzed, microwave assisted synthesis of new α -aminophosphonates as potential anti-diabetic agents: *In silico* ADMET and molecular docking study, *Org. Commun.* **2022**, *15*, 167-183.
- [29] Chen, J.-L.; Tang, W.; Che, J.-Y.; Chen, K.; Yan, G.; Gu, Y.-C.; Shi, D.-Q. Synthesis and Biological Activity Evaluation of Novel α -Amino Phosphonate Derivatives Containing a Pyrimidinyl Moiety as Potential Herbicidal Agents, *J. Agric. Food Chem.* **2015**, *63*, 7219-7229.
- [30] Rogacz, D.; Lewkowski, J.; Siedlerek, M.; Karpowicz, R.; Kowalczyk, A.; Rychter, P. The Effect of New Thiophene-Derived Diphenyl Aminophosphonates on Growth of Terrestrial Plants. *Materials* **2019**, *12*, 2018.
- [31] Reddy, N. M.; Poojith, N.; Mohan, G.; Reddy, Y. M.; Saritha, K. V.; Rao, P. V.; Reddy, A. V. K.; Swetha, V.; Zyryanov, G. V.; Krishna, B. S.; Reddy, C. S. Green synthesis, antioxidant activity, plant growth regulatory activity, molecular docking, QSAR, ADMET and bioactivity evaluation studies of novel α -furfuryl-2-alkylaminophosphonates. *ACS Omega* **2021**, *6*, 2934-2948.,
- [32] Zhang, S.; Zhang, M.-H.; Feng, S.; Zhang, W.-J.; Zhu, Y.-Y.; Li, Z.-W.; Bai, S. Research progress in agricultural bioactive phosphonate esters compounds. *Chem. Pap.* **2024**, *78*, 4045-4056.
- [33] Sravya, G.; Balakrishna, A.; Zyryanov, G. V.; Mohan, G.; Reddy, C. S.; Reddy, N. B. Synthesis of α -aminophosphonates by the Kabachnik-Fields reaction, *Phosphorus, Sulfur, and Silicon.* **2021**, *196*, 353-381.
- [34] Varga P. R.; Keglevich, G. Synthesis of α -aminophosphonates and related derivatives; The last decade of the Kabachnik-Fields reaction. *Molecules* **2021**, *26*, 2511.

Synthesis and antimicrobial activity of novel α -aminophosphonates

- [35] Fiore, C.; Sovic, I.; Lukin, S.; Halasz, I.; Martina, K.; Delogu, F.; Ricci, P. C.; Porcheddu, A.; Shemchuk, O.; Braga, D.; Pirat, J.-L.; Virieux, D.; Colacino, E. Kabachnik-Fields reaction by mechanochemistry: New horizons from old methods. *ACS Sustainable Chem. Eng.* **2020**, *8*, 18889-18902.
- [36] Mehraban, J. A.; Jalali, M. S.; Heydari, A. Formic acid catalyzed one-pot synthesis of α -aminophosphonates: An efficient, inexpensive and environmental friendly organocatalyst. *Chem. Pap.* **2018**, *72*, 2215-2223.
- [37] Ravi, N.; Venkatanarayana, M.; Sharathbabu, H.; Babu, K. R. Synthesis of Novel α -aminophosphonates by methanesulfonic acid catalyzed Kabachnik-Fields Reaction, *Phosphor. Sulfur Sil.* **2021**, *196*, 1018-1024.
- [38] Ceradini, D.; Shubin, K. One-pot synthesis of α -aminophosphonates by yttrium-catalyzed birum-oleksyszyn reaction, *RSC Adv.* **2021**, *11*, 39147-39152.
- [39] Rajkoomar, N.; Murugesan, A.; Robert, S. P.; Gengan M. Synthesis of methyl piperazinyl-quinolinyl α -aminophosphonates derivatives under microwave irradiation with Pd-SrTiO₃ catalyst and their antibacterial and antioxidant activities. *Phosphor. Sulfur Sil.* **2020**, *195*, 1031-1038.
- [40] Sreelakshmi, P.; Santhisudha, S.; Reddy, G. R.; Subbarao, Y.; Peddanna, K.; Apparao, C.; Reddy, C. S. Nano-CuO-Au-catalyzed solvent-free synthesis of α -aminophosphonates and evaluation of their antioxidant and α -glucosidase enzyme inhibition activities. *Synth. Commun.* **2018**, *48*, 1148-1163.
- [41] Piri, T.; Peymanfar, R.; Javanshir, S.; Amirnejat, S. Magnetic BaFe₁₂O₁₉/Al₂O₃: An efficient heterogeneous lewis acid catalyst for the synthesis of α -aminophosphonates (Kabachnik-Fields reaction). *Catal. Lett.* **2019**, *149*, 3384-3394.
- [42] Rasal, S. A.; Tamore, M. S.; Shimpi N. G. Ultrasound-mediated synthesis of novel α -aminophosphonates using graphene nanosheets-silver nanoparticles (GNS-AgNPs) as a recyclable heterogeneous catalyst. *ChemistrySelect* **2019**, *4*, 2293-2300.
- [43] Hajavazzade, R.; Mahjoub, A. R.; Kargarrazi, M. silica-coated MgAl₂O₄ nanoparticles supported phosphotungstic acid as an effective catalyst for synthesis of α -aminophosphonates. *Res. Chem. Intermed.* **2019**, *45*, 2341-2355.
- [44] Sreelakshmi, P.; Reddy, N. M.; Santhisudha, S.; Mohan, G.; Saichaitanya, N.; Sadik, S. M.; Peddanna, K.; Nagaraju, C.; Reddy, C. S. Nano Sb₂O₃ catalyzed green synthesis, cytotoxic activity and molecular docking study of novel α -aminophosphonates. *Med. Chem. Res.* **2019**, *28*, 528-544.
- [45] Sarfaraz, S.; Ishita, Y.; Ramana, M. M. V. Ultrasound assisted one-pot synthesis of novel antipyrine based α -aminophosphonates using TiO₂/carbon nanotubes nanocomposite as a heterogeneous catalyst. *Reac. Kinet. Mech. Cat.* **2021**, *134*, 917-936.
- [46] Olszewski, T. K. Environmentally benign syntheses of α -substituted phosphonates: Preparation of α -amino and α -hydroxyphosphonates in water, in ionic liquids, and under-solvent-free conditions. *Synthesis* **2014**, *46*, 403-429.
- [47] Ying, A.; Liu, S.; Yang, J.; Hu, H. Synthesis of α -amino phosphonates under a neat condition catalyzed by multiple-acidic ionic liquids. *Ind. Eng. Chem. Res.* **2014**, *53*, 16143-16147.
- [48] Shaikh, M. H.; Subhedar, D. D.; Khan, F. A. K.; Sangshetti J. N.; Shingate, B. B. [Et₃NH][HSO₄]-catalyzed one-pot, solvent-free synthesis and biological evaluation of α -aminophosphonates. *Res. Chem. Intermed.* **2016**, *42*, 5115-5131.
- [49] Eyckensa, D. J.; Henderson, L. C. Synthesis of α -aminophosphonates using solvate ionic liquids. *RSC Adv.*, **2017**, *7*, 27900-27904.
- [50] Boroujeni, K. P.; Shirazi, E. R.; Doroodmand, M. M. Synthesis of α -aminophosphonates using carbon nanotube supported imidazolium salt-based ionic liquid as a novel and environmentally benign catalyst. *Phosphor. Sulfur Sil.* **2016**, *191*, 683-688.
- [51] Razavia, N.; Akhlaghinia, B. Hydroxyapatite nanoparticles (HAp nanoparticles): A green and efficient heterogeneous catalyst for three-component one-pot synthesis of 2,3-dihydroquinazolin-4(1H)-one derivatives in aqueous media. *New J. Chem.* **2016**, *40*, 447-457.
- [52] Arnau, M.; Turon, P.; Alemán C.; Sans, J. Hydroxyapatite-based catalysts for CO₂ fixation with controlled selectivity towards C2 products. phenomenal support or active catalyst? *J. Mater. Chem. A*, **2023**, *11*, 1324-1334.
- [53] Murugesan, M.; Krishnamurthy, V.; Hebalkar, N.; Devanesan, M.; Nagamony, P.; Palaniappan, M.; Krishnaswamy, S.; Yuan, A. Nano-hydroxyapatite (HAp) and hydroxyapatite/platinum (HAp/Pt) core shell nanorods: Development, structural study, and their catalytic activity. *Canadian J. Chem. Eng.* **2021**, *99*, 268-280.
- [54] Munir, M. U.; Salman, S.; Ihsan, A.; Elsaman, T. Synthesis, characterization, functionalization and bio-applications of hydroxyapatite nanomaterials: An overview. *Int. J. Nanomed.* **2022**, *17*, 1903-925.
- [55] Fihri, A.; Len, C.; Varma, R. S.; Solhy, A. Hydroxyapatite: A review of syntheses, structure and applications in heterogeneous catalysis. *Coord. Chem. Rev.* **2017**, *347*, 48-76.

- [56] Nayak, B.; Samant, A.; Misra, P. K.; Saxena, M. Nanocrystalline Hydroxyapatite: a potent material for adsorption, biological and catalytic studies. *Materials Today: Proc.* **2019**, *9*, 689-698.
- [57] Amedlous, A.; Amadine, O.; Essamlali, Y.; Maati, H.; Semlal, N.; Zahouily, M. Copper loaded hydroxyapatite nanoparticles as eco-friendly fenton-like catalyst to effectively remove organic dyes. *J. Envir. Chem. Eng.* **2021**, *9*, 105501.
- [58] Block, J.; Beale, J. M. Wilson & *Gisvold's Textbook of Organic Medicinal and Pharmaceutical Chemistry.* **2003**
- [59] Edmond M. B. Wallace, S. E.; McClish, D. K.; Pfaller, M. A.; Jones, R.N.; Wenzel, R. P. Nosocomial bloodstream infections in united states hospitals: A three-year analysis. *Clin. Infect. Dis.* **1999**, *29*, 239-44.
- [60] Vijesh A.M.; Isloor, A.M.; Telkar, S.; Fun, H. K. Molecular docking studies of some new imidazole derivatives for antimicrobial properties. *Arabian J. Chem.* **2013**, *6*, 197-204.
- [61] Chmara, H.; Andruszkiewicz, R.; Borowski, E. Inactivation of glucosamine-6-phosphate synthetase from *salmonella typhimurium* It 2 sl 1027 by n β -fumarylcarboxyamido-1-2,3-diamino-propionic acid. *Biochem. Biophys. Res. Commun.* **1984**, *120*, 865-872.
- [62] Borowski E. Novel approaches in the rational design of antifungal agents of low toxicity. *Farmaco.* **2000**, *55*, 206-208.
- [63] Sadik, M. S.; Reddy, N. M.; Mohan, G.; Sreelakshmi, P.; Rajasekhar, A.; Rao, Ch. A.; Reddy, C. S. Green synthesis of diethyl((2-iodo-4-(trifluoromethyl)phenyl)amino)(aryl)methylphosphonates as potent α -glucosidase inhibitors. *Synth. Commun.* **2020**, *50*, 587-601.
- [64] Saikiran, A.; Nayak, B.V.; Mohan, G.; Murali, S.; Reddy, N. B.; Sravya, G.; Zyryanov, G. V.; Raju, C. N.; Reddy, C. S. Novel α -aminophosphonates of imatinib intermediate: synthesis, anticancer activity, human Abl tyrosine kinase inhibition and drug-likeness prediction. *Bioorg. Chem.* **2021**, *109*, 104718.
- [65] Dizdar, M.; Maksimovic, M.; Topcagic, A.; Avdic, M.; Vidic, D. Synthesis and bioactivity of 1-substituted tetrahydroisoquinolines derived from phenolic aldehydes. *Org. Commun.* **2023**, *16*, 197-203.
- [66] Singh, J.; Zaman, M.; K. Gupta, A. K. Evaluation of microdilution and disk diffusion methods for antifungal susceptibility testing of dermatophytes. *Medical Mycol.* **2007**, *45*, 595-602.
- [67] Tang, Y.Y.; Hu, X.Y.; Xu, F.; Xing, X. Chemical composition, antibacterial, synergistic antibacterial and cytotoxic properties of the essential oil from *Gelsemium elegans* (Gardner & Champ.) Benth., *Rec. Nat. Prod.* **2023**, *17*, 1074-1079.
- [68] Alam, M.; Kobir, M.E.; Kumer, A.; Chakma, U.; Akter, P.; Bhuiyan, M.M.H. Antibacterial, antifungal and antiviral activities of pyrimido [4,5-d]pyrimidine derivatives through computational approaches. *Org. Commun.* **2022**, *15*, 239-260.
- [69] Bommu, U. D.; Konidala, K. K.; Pabbaraju, N.; Yeguvapalli, S. Ligand-based virtual screening, molecular docking, qsar and pharmacophore analysis of quercetin-associated potential novel analogs against epidermal growth factor receptor. *J. Recep. Sign. Trans.* **2017**, *37*, 600-610.
- [70] Bommu, U. D.; Konidala, K. K.; Pabbaraju, N.; Yeguvapalli, S. QSAR modeling, pharmacophore-based virtual screening, and ensemble docking insights into predicting potential epigallocatechin gallate (EGCG) analogs against epidermal growth factor receptor. *J. Recep. Sign. Trans.* **2019**, *39*, 18-27.
- [71] Konidala, K. K.; Bommu, U. D.; Yeguvapalli, S. et al. *In silico* insights into prediction and analysis of potential novel pyrrolopyridine analogs against human MAPKAPK-2: a new SAR-based hierarchical clustering approach. *3 Biotech* **2018**, *8*, 385.

ACG
publications

© 2024 ACG Publications